Molecular basis of the head-to-tail assembly of the giant muscle proteins obscurin-like 1 and titin

SUPPLEMENT

Florian Sauer, Juha Vahokoski, Young-Hwa Song & Matthias Wilmanns

EMBL-Hamburg, Notkestrasse 85, D-22603 Hamburg, Germany

Correspondence: Matthias Wilmanns

Email: wilmanns@embl-hamburg.de

Phone: +49-40-899020-126

Fax: +49-40-89902-149

Materials and Methods

X-ray structure determination. Prior to X-ray data collection, homogeneous Obsl1(Ig1)-titin(M10) complex crystals were separated from clusters with a needle, soaked in cryoprotectant solution (20% [v/v] glycerol, with or without 0.5 M LiBr) for 1 min, and flash-frozen to 100K in the cryo-stream. Three sets of X-ray diffraction data were collected at the tunable beamline X12 (EMBL/DESY, Hamburg, Germany). The first two data sets were from crystals soaked with LiBr and were obtained at wavelengths optimized to obtain an anomalous signal at the bromine peak and inflection points. The third data set was taken from native Obsl1(Ig1)-titin(M10) complex crystals. All data sets were integrated, merged and scaled with the XDS/XSCALE (Kabsch, 1993).

The structure was solved by the multiple anomalous dispersion method at two different wavelengths, using several software modules of the SHELX phasing and structure refinement package (Sheldrick, 2008), integrated into the Auto-Rickshaw platform (Panjikar et al, 2005). FA values were calculated with the program SHELXC. The maximum resolution for sub-structure determination and initial phase calculation was set to a resolution limit 2.0 Å. A total of 15 bromide ions were found with the program SHELXD. The correct hand of the substructure was determined with the programs ABS (Hao, 2004) and SHELXE. Initial phases were calculated after density modification with the program SHELXE. An initial model containing 178 of 207 residues was built in ARP/wARP (Morris et al, 2003) and the model was manually completed using COOT (Emsley & Cowtan, 2004). Final refinement of the coordinates and individual B-factors against high-resolution native X-ray data was carried out with PHENIX.refine (Version 1.5-2) (Zwart et al, 2008). Further X-ray data and refinement statistics are listed in **Table 1**. Because of the high resolution of the diffraction data, a total of 25 residues were fitted with alternative conformations. Interface areas were calculated and characterized with the program AREAIMOL from the CCP4 suite (Collaborative Computational Project, 1994). Structural relationships between titin(M10) and Obsl1(Ig1) were analyzed with SSM (Krissinel & Henrick, 2004). All structural figures were created with the Pymol software (http://www.pymol.org/).

FRET analysis

For Foerster Resonance Energy Transfer (FRET) measurements, purified Obsl1(Ig1) and Obs(Ig1) were N-terminally labeled with Alexa Fluor 488 tetrafluorophenyl ester (donor probe). The titin(M10) domain was labeled wit Alexa Fluor 647 succinimidyl ester (acceptor probe), according to the manufacturer's protocols (Invitrogen). For a positive control experiment, Obsl1(Ig1) was labeled at the surface exposed Cys15 with Alexa Fluor 488 C_5-maleimide (donor probe) and with Alexa Fluor 488 succinimidyl ester (acceptor probe) at the N-terminus. N-terminal labeling was carried out at a concentration of 0.4 mM protein in 100 mM $NaHPO_4$ (pH 8.0), 150 mM NaCl. Cysteine labeling was carried out in 100 mM PBS (pH 7.2). All Alexa Fluor Dyes ware incubated in a four-fold molar excess for 12h at 4°C. The reaction was quenched by addition of Tris/HCl (pH 7.0). Subsequently, the remaining free dye was removed, using a desalting column and labeled protein samples were re-buffered into 100 mM PBS (pH 7.2). Final Protein concentrations and labeling efficiencies were determined by measurements of the sample extinction at wavelengths of 495 nm (Alexa Fluor 488), 650 nm (Alexa Fluor 647) and 280 nm.

For FRET measurements, proteins at a final concentration of 1 uM were mixed in a 1:1 ratio. The following samples were obtained after labeling: 1, D(N)-Obsl1(Ig1) – A(N)-titin(M10); 2, D(N)-Obs1(Ig1) – A(N)-titin(M10); 3, A(N)-D(Cys15)-Obsl1(Ig1) – titin(M10), and all three FRET variants only with donor fluorophore label in complex with non-labeled titin(M10). The FRET measurements were performed using Fluorolog3 (Horiba Jovin Yvon). For each sample, an emission spectrum was recorded, and the FRET and donor samples were excited at 495 nm. The fluorescence spectra of the donor samples were normalized onto the spectra of the FRET-samples. Subsequently, the fluorescence intensities of FRET samples were subtracted from the normalized donor spectra and relative fluorescence intensities were plotted. For the calculation of distances, the FRET samples were also recorded with the excitation at 650 nm, corresponding to the direct excitation of the acceptor dye. The energy transfer efficiency was calculated with the method of Clegg (Clegg, 1992) and subsequently used for distance calculation.

Supplement Figure 1: Obsl1(Ig1)/Obs(Ig1)-Titin(M10) complex formation. A and B, normalized gel filtration elution profiles of Obsl1(Ig1)-Titin(M10), Obs(Ig1)-Titin(M10) and separate domains; C, SDS-PAGE analysis of the same complexes and separate domains. In the elution profiles, those protein fractions that have been used for SDS-PAGE analysis are indicated with dashed lines.

Supplement Figure 2: FRET measurements. FRET spectra, showing relative fluorescence intensities of Obs(Ig1)/Obsl1(Ig1)–titin(M10) complexes, N-terminally labeled with donor and acceptor dye. The estimated FRET distances for Obsl1(Ig1, N-terminus)-titin(M10, N-terminus) and Obs1(Ig1, N-terminus)-titin(M10, N-terminus) are 36.7 ± 1.6 A and 48.2 ± 3.0 A, respectively. These values match with the measured distance of 48 Å for the visible N-termini of the two Ig domains in the X-ray structure of the Obsl1(Ig1)-titin(M10) complex. Since the first nine residues of Obsl1(Ig1) are not visible, we also carried out a control experiment, using a double labeled Obsl1(Ig1) sample, with the acceptor fluorophore at the N-terminus and donor fluorophore at Cys15, and unlabeled titin(M10) domain. The FRET efficiency is the highest among all measured samples, indicating a very short distance between the labels. However, since the labeling efficiency could not precisely determined, we did not calculate an experimental FRET distance. Nevertheless, the experiment shows that the N-terminal tail of Obsl1 (residues 1-9) that is invisible in the X-ray structure seems to remain in the close vicinity of the visible N-terminus of Obsl1 (Gln10). Overall, the FRET data support the antiparallel arrangement of Obsl1(Ig1)–titin(M10), observed in the X-ray structure of the complex, and further demonstrate that the overall architecture of the Obsl1(Ig1)–titin(M10) and Obs(Ig1)–titin(M10) complexes are similar. These data are further supported by the binding affinity data from several point mutations (Table 2).

Supplement Figure 3: Sample ITC measurements of Obs(Ig1)/Obsl1(Ig1)-titin(M10) complex formation. A, Obsl1(Ig1)-titin(M10); B, Obs(Ig1)-titin(M10). The upper panel shows the raw data measured in μcal/sec. The lower panel shows the absorbed heat per injection in kcal/mol, determined by calculation of the peak surface and corrected for residual heat absorption after

complex saturation.

Supplement Figure 4: Circular dichroism spectra of titin(M10) variants (*cf*. Table 2). Upper panel: titin(M10,wt) as reference, titin(M10,V22P), titin (M10,D61R); lower panel: titin(M10,wt) as reference, titin(M10,H55P), titin(M10,I56N), titin(M10,L65P). Experimental errors are indicated with vertical bars.

Supplement Figure 5:Localization of known titin(M10) mutations from TMD patients. Ribbon drawing of the structure of the Obsl1(Ig1)-titin(M10) complex (*cf.* Figure 2A, rotated by about 180 deg. around a vertical axis in the paper plane, to optimize visualization of residue mutations in TMD patients). The side chains of residues from those TMD mutations experimentally investigated in this contribution are shown in light green and are labeled. The side chains of the Finnish TDM mutation, affecting residues 36-39, are shown in light magenta. The side chain of Trp39 points into the hydrophobic core of titin(M10). The cartoon smooth option in this figure representation was disabled, to keep the side chains connected to secondary structural elements.

References:

Clegg RM (1992) Fluorescence resonance energy transfer and nucleic acids. *Methods Enzymol* 211: 353-388

Collaborative Computational Project N (1994) The CCP4 Suite: Programs for Protein Crystallography. *Acta Cryst* D50: 760-763.

Emsley P, Cowtan K (2004) Coot: model-building tools for molecular graphics. *Acta Crystallogr D Biol Crystallogr* 60(Pt 12 Pt 1): 2126-2132

Hao Q (2004) ABS: a program to determine absolute configuration and evaluate anomalous scatterer substructure. *Journal of Applied Crystallography* 37(3): 498-499

Kabsch W (1993) Automatic processing of rotation diffraction data from crystals of initially unknown symmetry and cell constants. *J Appl Cryst* 26: 795-800

Krissinel E, Henrick K (2004) Secondary-structure matching (SSM), a new tool for fast protein structure alignment in three dimensions. *Acta Crystallogr D Biol Crystallogr* 60(Pt 12 Pt 1): 2256-2268

Morris RJ, Perrakis A, Lamzin VS (2003) ARP/wARP and automatic interpretation of protein electron density maps. *Methods Enzymol* 374: 229-244

Panjikar S, Parthasarathy V, Lamzin VS, Weiss MS, Tucker PA (2005) Auto-Rickshaw: an automated crystal structure determination platform as an efficient tool for the validation of an X-ray diffraction experiment. *Acta Crystallogr D Biol Crystallogr* 61(Pt 4): 449-457

Sheldrick GM (2008) A short history of SHELX. *Acta Crystallogr A* 64(Pt 1): 112-122

Zwart PH, Afonine PV, Grosse-Kunstleve RW, Hung LW, Ioerger TR, McCoy AJ, McKee E, Moriarty NW, Read RJ, Sacchettini JC, Sauter NK, Storoni LC, Terwilliger TC, Adams PD (2008) Automated structure solution with the PHENIX suite. *Methods Mol Biol* 426: 419-435

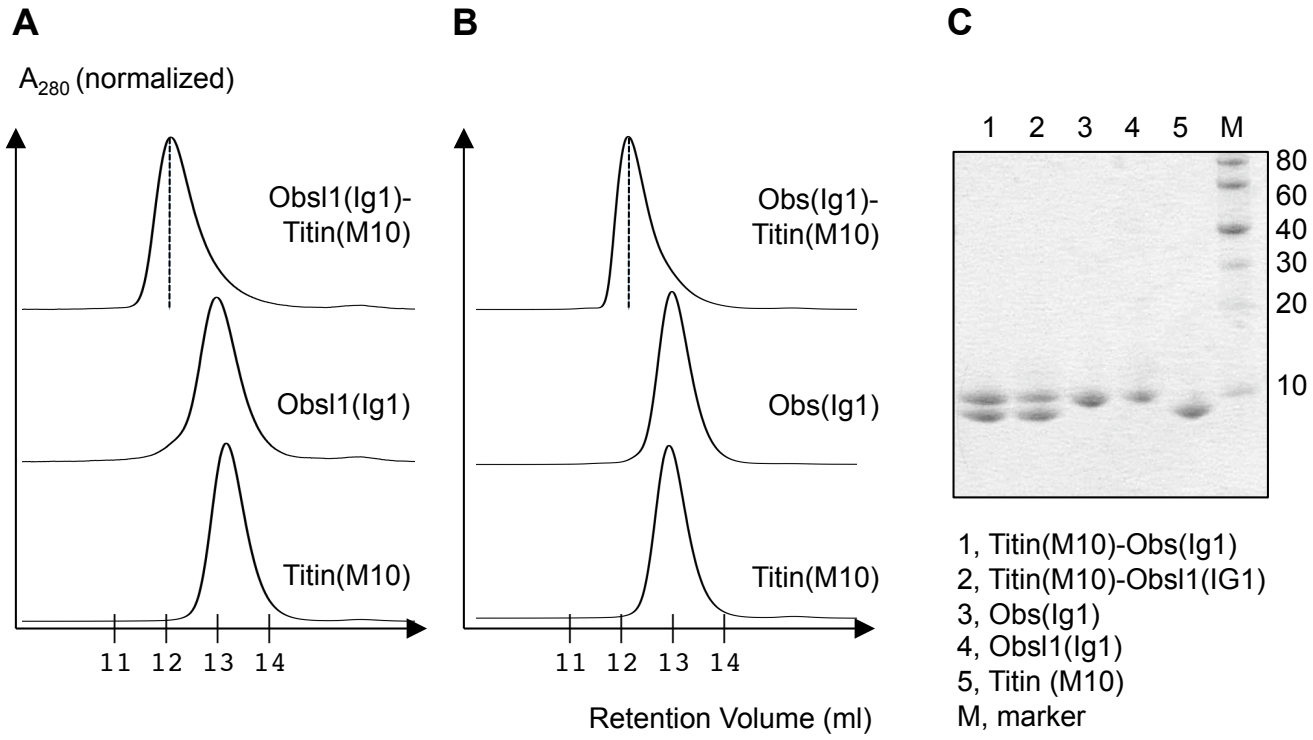

Supplement Figure 1

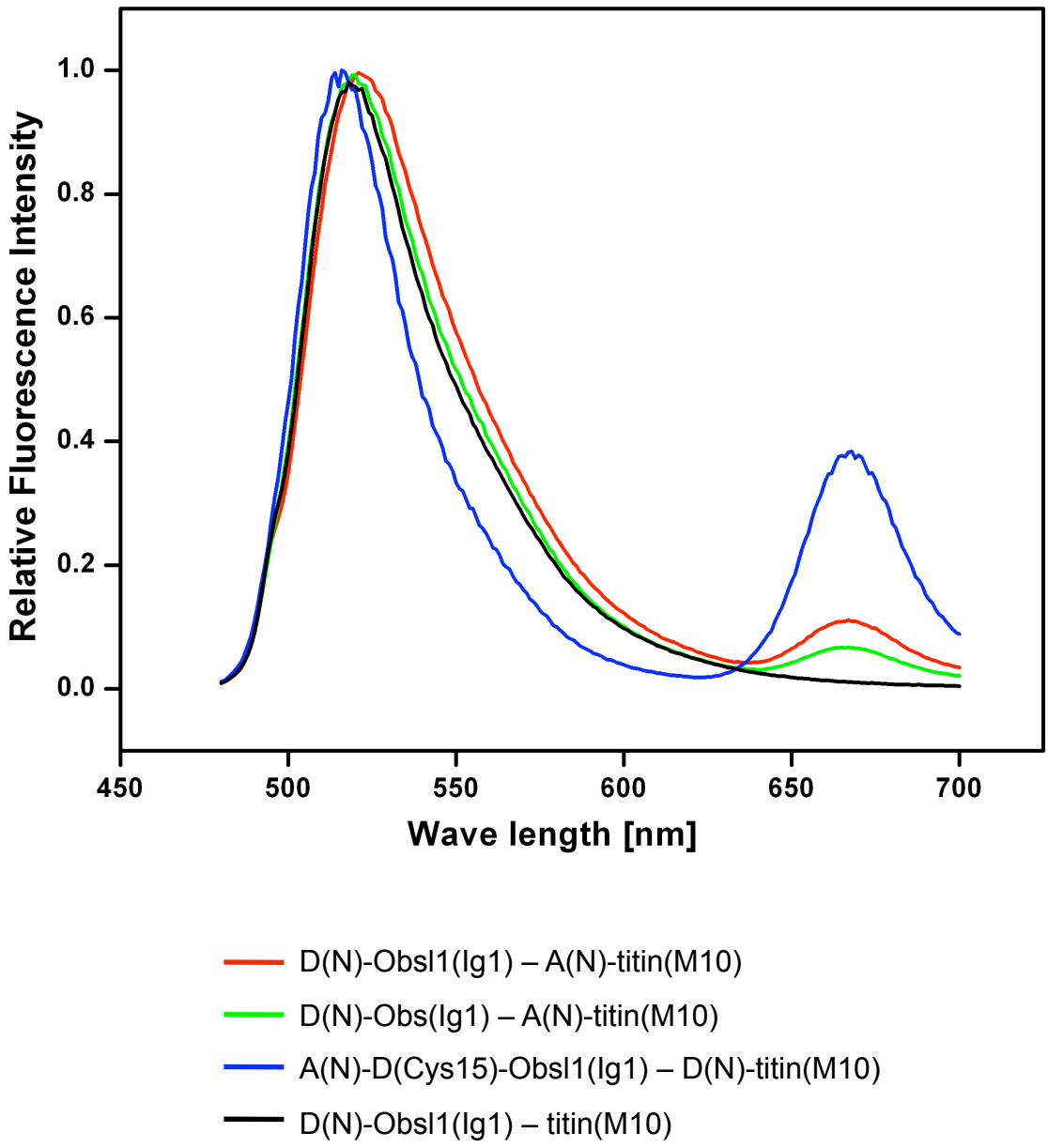

Supplement Figure 2

A) ObsI1(Ig1)-Titin(M10)

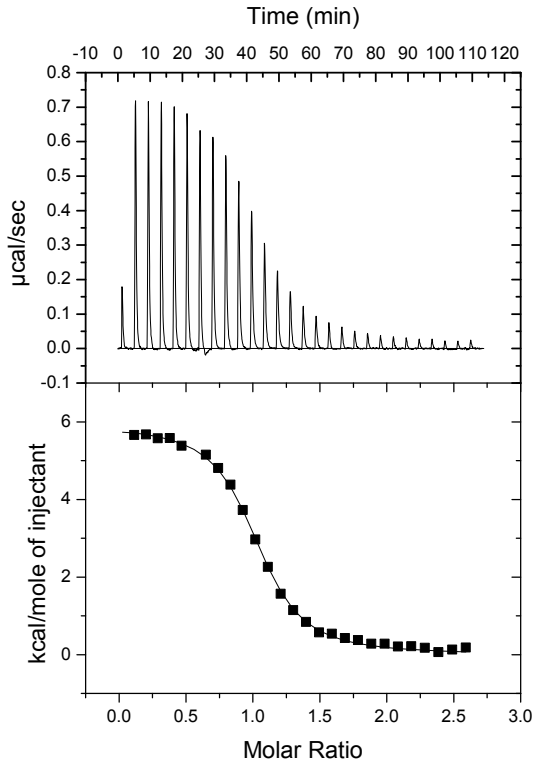

B) Obs(Ig1)-Titin(M10)

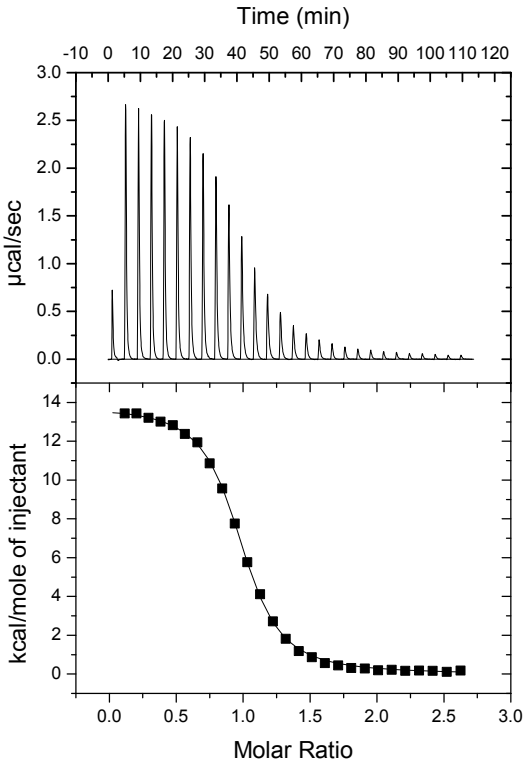

Supplement Figure 3

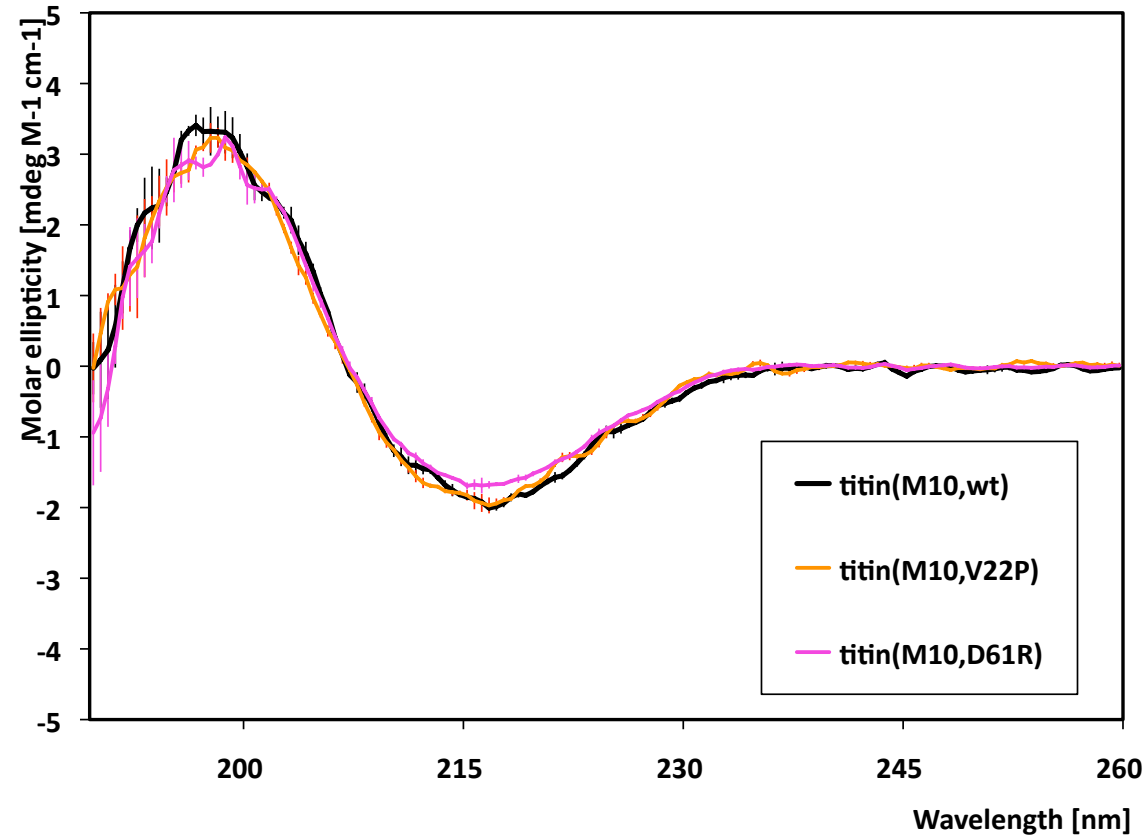

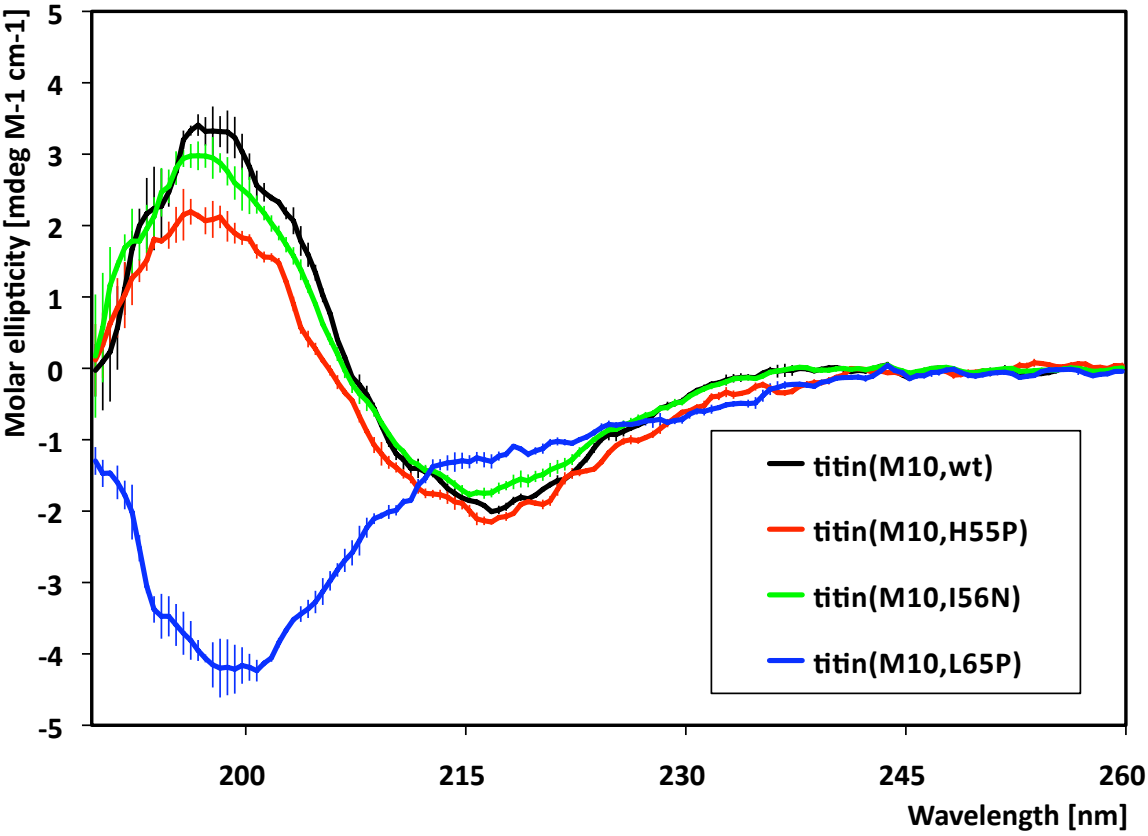

Supplement Figure 4

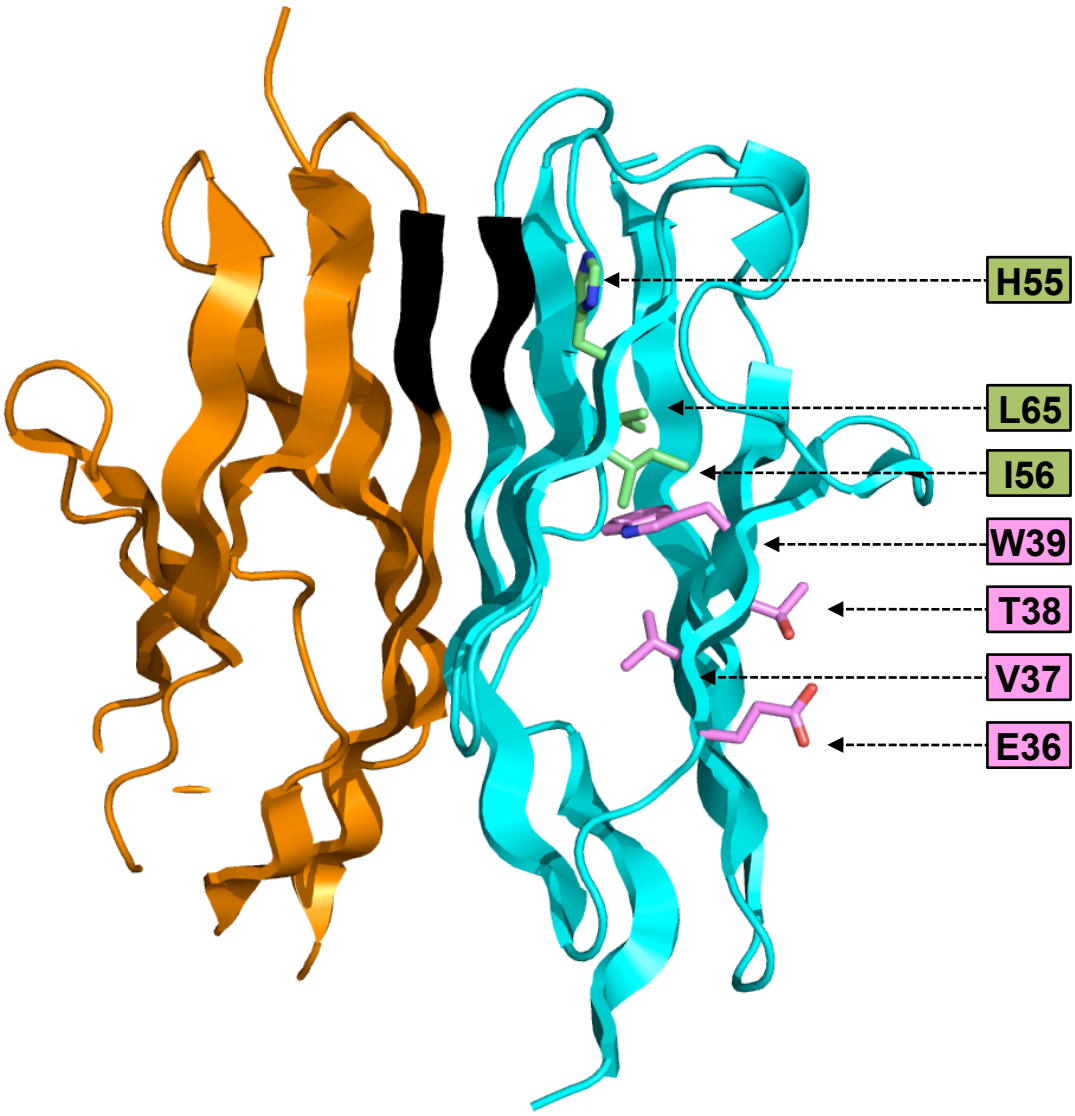

Supplement Figure 5